Structure of Concentrated Aqueous Sodium Formate Solutions

Yasuo Kameda,* Takahiro Mori, Takashi Nishiyama, Takeshi Usuki, and Osamu Uemura

Department of Material and Biological Chemistry, Faculty of Science, Yamagata University, Kojirakawa-machi 1-4-12, Yamagata 990

(Received November 14, 1995)

Time-of-flight neutron and X-ray diffraction as well as Raman spectroscopic measurements were carried out on an aqueous 15 mol% HCOONa solution in order to investigate the hydration structure of both the formate and sodium ions in the concentrated aqueous solution. The intramolecular bond distances of $DCOO^-$ ($r_{CD}=1.07\pm0.01$ Å, $r_{CO}=1.272\pm0.007$ Å and $r_{OO}=2.18\pm0.02$ Å) were determined through a least-squares fit of the observed neutron interference term in the high-Q region. The average hydrogen-bond distances between the D_2O molecules in the solution ($r(O\cdots D)=1.92\pm0.02$ Å and $r(D\cdots D)=2.42\pm0.02$ Å) were also obtained. The hydration parameters on the formate ion were estimated to be $r_{O_{formate}\cdots H_2O}=2.82\pm0.01$ Å and $n_{O_{formate}\cdots H_2O}=4.4\pm0.2$ from a least-squares fit of the X-ray intermolecular interference term. A preferred orientation between the formate ion and hydrated water molecules was suggested from the present X-ray data. The hydration number of Na^+ in the solution was given to be 4.6 ± 0.2, besides the intermolecular distance ($r_{Na^+\cdots H_2O}=2.37\pm0.01$ Å). The symmetrical stretching vibrational band of the hydrated sodium ion, $Na^+(H_2O)_n$, in a 15 mol% HCOONa solution was observed at 225 cm^{-1} in the present isotropic Raman spectrum.

Studies of the formate ion, $HCOO^-$, have occupied an important position in the field of coordination chemistry, because of its versatile coordination behavior. A number of facultative complexes having $HCOO^-$ as the ligand have been synthesized, and the crystalline structures of these complexes have been extensively clarified.[1] On the other hand, the structure of aqueous solutions including the formate ion–metal complexes, and the hydration structure of $HCOO^-$, itself, in solution have been reported only a little (as described below).

Edwards and Knowles have pointed out from their Raman spectroscopic study that $HCOO^-$ does not exhibit complex formation with Ni^{2+} in an aqueous 2 mol dm^{-3} $(HCOO)_2Ni$ solution.[2] The polarized Raman spectra in a concentrated aqueous HCOONa solution (6 mol kg^{-1}) have suggested that $HCOO^-$ has a planer molecular structure in aqueous solution.[3,4] An X-ray diffraction study of an aqueous 10.77 mol dm^{-3} HCOOTl solution has suggested the formation of the tetramer for $HCOO^-$, $Tl_4(O_2CH)_4$, in solution.[5] A Monte-Carlo simulation for a system containing one $HCOO^-$ and 256 H_2O molecules has predicted that the number of H_2O molecules hydrogen-bonded to the oxygen atom of $HCOO^-$ is ca. 7 per $HCOO^-$.[6] A further accumulation of structural data is presently needed to elucidate the exact hydration structure of the formate ion in aqueous solution.

In the present paper we report on results concerning the time-of-flight (TOF) neutron and X-ray diffractions, and polarized Raman scattering measurements of an aqueous 15 mol% HCOONa solution. Information concerning the intramolecular structure of $HCOO^-$ and the intermolecular hydrogen-bonded structure in solution have been determined by a least-squares fitting analysis of the observed neutron interference term. Moreover, the hydration structure of Na^+ in a concentrated aqueous solution was also investigated using the results of X-ray diffraction data with the help of low-frequency isotropic Raman spectra.

Experimental

Neutron Diffraction Measurement. A fully deuterated aqueous 15 mol% DCOONa solution was prepared by dissolving the required amount of DCOONa (99.0% D, MSD ISOTOPES) into D_2O (99.8% D, Aldrich Chemical Co., Inc.). A sample solution was sealed in a cylindrical quartz sample cell (7.3 mm in inner diameter and 0.5 mm in thicknesss). A TOF neutron-diffraction measurement was carried out at 25 °C using the HIT-II spectrometer[7] installed at the pulsed-spallation neutron source (KENS) at the National Laboratory for High Energy Physics (KEK), Tsukuba, Japan. Measurements on an empty cell, background and a vanadium rod having the same dimensions as that of the sample, were made in advance.

X-Ray Diffraction Measurement. X-Ray diffraction with Mo $K\alpha$ radiation ($\lambda=0.7107$ Å) was measured at 25 °C on a 15 mol% HCOONa solution under the reflection geometry using a $\theta-\theta$ X-ray diffractometer manufactured by Rigaku Co. The isotopic compositions of the constituent atoms in the sample were all natural abundances. The scattered X-ray intensities from the sample were counted at an interval of 0.2° over an angular range of $3°\leqq 2\theta \leqq 150°$, corresponding to the scattering vector range, $0.5\leqq Q\leqq 17.1$ Å^{-1} ($Q=4\pi \sin\theta/\lambda$), with a fixed counting time of 40 s. The whole angular range was scanned eight times in order to keep good statistics for the scattering data, and to minimize any long-term instrumental drift. The total number of counts reached at least 1.5×10^5, and amounted, on the average, to as much as 3.5×10^6 counts. Details concerning the X-ray diffraction measurement were previously described.[8]

Raman Scattering Measurement. Sample solutions of 5 and 15 mol% HCOONa were prepared by dissolving a weighted

amount of anhydrous HCOONa (Nacalai Tesque Inc., Guaranteed grade) in distilled water and in D_2O (99.8% D, Aldrich Chemical Inc., Co.). Aqueous 5 and 10 mol% NaCl and NaBr solutions were also prepared by dissolving dried anhydrous salts (Nacalai Tesque Inc., Guaranteed grade) in distilled water for a Raman-scattering measurement. All of the solutions were filtered through a 0.45 μm Teflon® millipore filter before introducing them into a Pyrex® Raman cell (10×10 mm, 40 mm H), so as to remove any dust particles. The polarized Raman spectra were recorded at 25 °C in the frequency range of $30 \leqq \nu \leqq 1000$ cm^{-1} using a JASCO NR-1100 spectrometer with a 514.5 nm line of an NEC GLG-3200 Ar^+ laser operated at 200 mW. The details concerning the Raman-scattering measurement are completely identical to those described in our previous papers.[9,10]

Data Reduction

Neutron Diffraction Data. The observed scattering intensities from the sample were corrected for any background and absorption[11] as well as multiple[12] and incoherent scattering. The corrected intensities were then converted to the absolute scale using scattering intensities from a vanadium rod. The scattering data from 66 sets of lower scattering-angle detectors located at $10 \leqq 2\theta \leqq 51°$ were combined so as to minimize the inelasticity-distortion effect for the observed scattering cross section, and then employed for a subsequent analysis. A correction for any low-frequency systematic error was also applied in the same way as that described in our previous paper.[13]

The observed total-interference term, scaled by the stoichiometric unit, $(DCOONa)_x\,(D_2O)_{1-x}$, can be divided into two contributions, namely, the intra- and intermolecular interference terms:

$$i_N(Q) = i_N^{intra}(Q) + i_N^{inter}(Q), \tag{1}$$

where

$$i_N^{intra}(Q) = x \cdot i_N^{intra}(Q)\,(\text{for } DCOO^-) + (1-x) \cdot i_N^{intra}(Q)\,(\text{for } D_2O), \tag{2}$$

$$\begin{aligned} i_N^{intra}(Q)\,(\text{for } DCOO^-) = {} & 2b_C b_D \exp(-l_{CD}^2 Q^2/2)\sin(Qr_{CD})/(Qr_{CD}) \\ & + 4b_C b_O \exp(-l_{CO}^2 Q^2/2)\sin(Qr_{CO})/(Qr_{CO}) \\ & + 4b_O b_D \exp(-l_{OD}^2 Q^2/2)\sin(Qr_{OD})/(Qr_{OD}) \\ & + 2b_O^2 \exp(-l_{OO}^2 Q^2/2)\sin(Qr_{OO})/(Qr_{OO}) \end{aligned} \tag{3}$$

and

$$\begin{aligned} i_N^{intra}(Q)\,(\text{for } D_2O) = {} & 4b_O b_D \exp(-l_{OD}'^2 Q^2/2)\sin(Qr_{OD}')/(Qr_{OD}') \\ & + 2b_D^2 \exp(-l_{DD}'^2 Q^2/2)\sin(Qr_{DD})/(Qr_{DD}). \end{aligned} \tag{4}$$

Here, b_i, l_{ij}, and r_{ij} denote the coherent-scattering length of atom i, the root-mean-square amplitude and the internuclear distance of the i–j pair, respectively. Contributions from the nearest-neighbor intermolecular O···D and D···D correlations in Q-space, which give direct information concerning the intermolecular hydrogen-bonded structure in the solution, were evaluated as follows (assuming the Gaussian distribution):

$$\begin{aligned} i_N^{inter}(Q)\,(\text{for O}\cdots\text{D}) = {} & 2c_O n_{OD} b_O b_D \exp(-l_{OD}''^2 Q^2/2) \\ & \times \sin(Qr_{OD}'')/(Qr_{OD}'') \end{aligned} \tag{5}$$

and

$$\begin{aligned} i_N^{inter}(Q)\,(\text{for D}\cdots\text{D}) = {} & c_D n_{DD} b_D^2 \exp(-l_{DD}'^2 Q^2/2) \\ & \times \sin(Qr_{DD}')/(Qr_{DD}'), \end{aligned} \tag{6}$$

where, c_i and n_{ij} indicate the number of atom i and the coordination number of the i–j pair, respectively. The correlations of the $Na^+\cdots O$ and $Na^+\cdots D$ pairs (described below) are also included in the model function, although they seem to contribute only slightly to the total interference function:

$$\begin{aligned} i_N^{inter}(Q)\,(\text{for Na}^+\cdots\text{O}) = {} & 2c_{Na} n_{NaO} b_{Na} b_O \exp(-l_{NaO}^2 Q^2/2) \\ & \times \sin(Qr_{NaO})/(Qr_{NaO}) \end{aligned} \tag{7}$$

and

$$\begin{aligned} i_N^{inter}(Q)\,(\text{for Na}^+\cdots\text{D}) = {} & 2c_{Na} n_{NaD} b_{Na} b_D \exp(-l_{NaD}^2 Q^2/2) \\ & \times \sin(Qr_{NaD})/(Qr_{NaD}). \end{aligned} \tag{8}$$

A least-squares fitting analysis of the observed total-interference term in the range of $6.0 \leqq Q \leqq 32.0$ Å^{-1} was made using the following theoretical model function:

$$\begin{aligned} i_N^{calc}(Q) = {} & i_N^{intra}(Q)\,(\text{for } DCOO^- \text{ and } D_2O) \\ & + i_N^{inter}(Q)\,(\text{for O}\cdots\text{D, D}\cdots\text{D, Na}^+\cdots\text{O, and Na}^+\cdots\text{D pairs}). \end{aligned} \tag{9}$$

The fitting procedure was performed using the SALS program,[14] while assuming that statistical errors uniformly distribute over the entire range of Q covered.

The neutron total-distribution function ($g_N(r)$) can be given by the Fourier transform of $i_N(Q)$ according to

$$g_N(r) = 1 + (2\pi^2\rho r)^{-1} \left(\sum c_i b_i\right)^{-2} \int_0^{Q_{max}} Q i_N(Q) \sin(Qr)\mathrm{d}Q, \tag{10}$$

where ρ denotes the number density of the stoichiometric unit, $(DCOONa)_x(D_2O)_{1-x}$. The upper limit of the integral (Q_{max}) in the present study was set to be 32.0 Å^{-1}.

X-Ray Diffraction Data. The correction and normalization procedures for the observed X-ray intensities were almost similar to those given in our previous paper.[8] The observed X-ray total interference term ($i_X(Q)$) is

$$i_X(Q) = (I_{eu}(Q) - \langle f^2 \rangle)/\langle f \rangle^2, \tag{11}$$

where

$$\langle f^2 \rangle = \sum c_i [(f_i(Q) + f_i')^2 + f_i''^2] \tag{12}$$

and

$$\langle f \rangle^2 = \left[\sum c_i (f_i(Q) + f_i')\right]^2 + \left[\sum c_i f_i''\right]^2. \tag{13}$$

Here, $I_{eu}(Q)$ expresses the normalized coherent-scattering intensity in electron units, and $f_i(Q)$ corresponds to the atomic scattering factor of atom i. The real and imaginary parts for the anomalous dispersion factor are given by f_i' and f_i'', respectively. The X-ray distribution function ($g_X(r)$) can be evaluated by a Fourier transform of $i_X(Q)$ with an upper integral limit of Q: $Q_{max} = 17.1$ Å^{-1};

$$g_X(r) = 1 + (2\pi^2\rho r)^{-1}\int_0^{Q_{max}} Qi_X(Q)\sin(Qr)dQ. \quad (14)$$

The observed total X-ray interference term, scaled by the stoichiometric unit, $(HCOONa)_x(H_2O)_{1-x}$, can also be represented by the sum of the intra- and intermolecular interference terms,

$$i_X(Q) = i_X^{intra}(Q) + i_X^{inter}(Q), \quad (15)$$

where

$$i_X^{intra}(Q) = x\cdot i_X^{intra}(Q)\ (\text{for } HCOO^-) + (1-x)\cdot i_X^{intra}(Q)\ (\text{for } H_2O). \quad (16)$$

The X-ray intramolecular interference terms for $HCOO^-$ and H_2O can be derived from Eqs. 3 and 4, respectively, by substituting the atomic scattering factor for X-rays ($f_i(Q)$) for the neutron coherent scattering length (b_i). In the present analysis, $i_X^{intra}(Q)$ was evaluated by using the interatomic distances and their root-mean-square displacements for both the formate ions and the water molecules in the solution, which were already determined in a neutron data analysis. The calculated $i_X^{intra}(Q)$ was then subtracted from the observed $i_X(Q)$ term to obtain the intermolecular interference term, $(i_X^{inter}(Q))$.

The theoretical intermolecular interference term ($i_X^{calc}(Q)$) was calculated by summing the nearest-neighbor short-range interaction ($i_X^s(Q)$) and the long-range interaction ($i_X^l(Q)$) for all possible atom pairs in the solution,

$$i_X^{calc}(Q) = i_X^s(Q) + i_X^l(Q), \quad (17)$$

where

$$i_X^s(Q) = \sum i_{ij}(Q) \quad (18)$$

and

$$i_{ij}(Q) = (2-\delta_{ij})c_i n_{ij}[(f_i(Q)+f_i')(f_j(Q)+f_j') + f_i''f_j'']\times\exp(-l_{ij}^2Q^2/2)\sin(Qr_{ij})/(Qr_{ij})/\langle f\rangle^2 \quad (19)$$

$$\begin{cases}\delta_{ij} = 1\ (i=j)\\ \delta_{ij} = 0\ (i\neq j).\end{cases}$$

The long-range interaction was evaluated using the following equation:[15—17]

$$i_X^l(Q) = 4\pi\rho_0\sum c_ic_j[(f_i(Q)+f_i')(f_j(Q)+f_j') + f_i''f_j'']\times\exp(-l_{0ij}^2Q^2/2)[Qr_{0ij}\cos(Qr_{0ij}) - \sin(Qr_{0ij})]Q^{-3}/\langle f\rangle^2, \quad (20)$$

where, r_{0ij} denotes the distance beyond which a continuous distribution of j atoms around atom i is assumed. The parameter l_{0ij} describes the sharpness of the boundary at r_{0ij}. The parameters n_{ij}, l_{ij}, and r_{ij} in Eq. 19, and l_{0ij} and r_{0ij} in Eq. 20 were determined through a least-squares fit of Eq. 17 to the observed $i_X^{inter}(Q)$. The fitting procedure was performed in the $1.0\leqq Q\leqq 17.1$ Å^{-1} range using the SALS program.[14]

Raman Scattering Data. A correction of the observed Raman spectra for the Bose–Einstein factor, which is needed to distinguish the low-frequency components, was made using the following equation:[18—21]

$$I^{corrected}(\nu) = (\nu_0-\nu)^{-4}\cdot\nu\cdot[1-\exp(-h\nu/kT)]\cdot I^{obs}(\nu), \quad (21)$$

where ν and ν_0 are the Stokes–Raman shift and the wavenumber of the incident light, respectively. The isotropic Raman intensity ($I^{iso}(\nu)$) can be obtained using

$$I^{iso}(\nu) = I^{\parallel}(\nu) - 4/3\cdot I^{\perp}(\nu), \quad (22)$$

where $I^{\parallel}(\nu)$ and $I^{\perp}(\nu)$ denote the corrected parallel and perpendicular spectra, respectively. A peak analysis of the isotropic spectra was carried out with the SALS program,[14] assuming a Gaussian-type peak function.

Results and Discussion

The least-squares fit for the observed neutron total-interference term ($i_N(Q)$) is shown in Fig. 1. A satisfactory agreement was obtained between the observed and calculated $i_N(Q)$ in the $6.0\leqq Q\leqq 32.0$ Å^{-1} range. Figure 2 gives the neutron distribution function ($g_N(r)$), evaluated by a Fourier transform of the observed $i_N(Q)$. The sharp peak at $r\approx 1$ Å is attributed to an intramolecular O–D interaction within the D_2O molecule. The intramolecular C–D interaction within $DCOO^-$ must be involved in this peak. Periodic ripples occurring at $r<0.8$ Å and $1.2<r<3.0$ Å in $g_N(r)$ may possibly be due to a termination error and/or the statistical uncertainty in the observed $i_N(Q)$ in the high-Q region. Contributions from the $Na^+\cdots O$ and $Na^+\cdots D$ pairs in $g_N(r)$ may appear as a very small peak at around $r\approx 3$ Å.

The fitting result of the observed $i_N(Q)$ is summarized in Table 1. The present value of the intramolecular C–O distance within $DCOO^-$ ($r_{CO}=1.272\pm0.007$ Å) is in reasonable agreement with that reported by X-ray diffraction studies for crystalline HCOONa ($r_{CO}=1.27$ Å,[22] 1.246 Å[23]) and HCOOK ($r_{CO}=1.2426$ Å,[24] 1.242 Å[25]). The present value of r_{CD} (1.07±0.01 Å) also agrees with that in pure liquid formic acid based on a neutron-diffraction study ($r_{CD}=1.10$ Å[26])

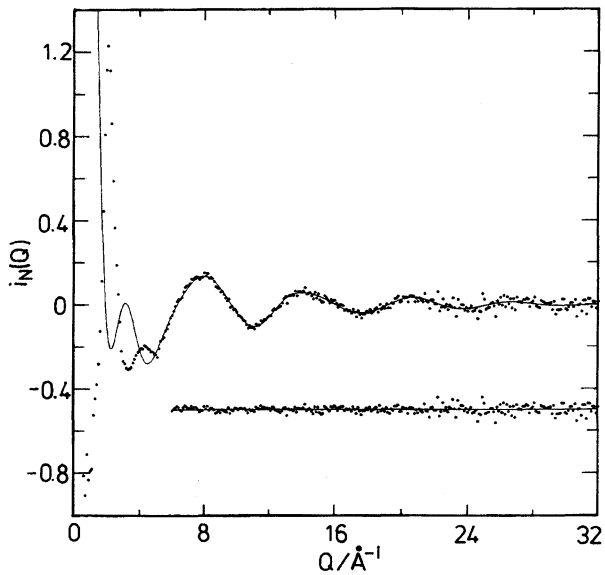

Fig. 1. The observed neutron total interference term (dots) and the best fit with the theoretical interference term of Eq. 9 (solid line) for aqueous 15 mol% DCOONa solution in D_2O. The residual function (dots) is shown below.

Table 1. Results of the Least-Squares Refinements for the Neutron Interference Term of Aqueous 15 mol% DCOONa Solution in D_2O[a)]

	Interaction	r_{ij}/Å	l_{ij}/Å	n_{ij}
Intramolecular	C–D	1.07(1)	0.07(2)	1.0[b)]
Structure	C–O	1.272(7)	0.05(1)	2.0[b)]
$DCOO^-$	O···O	2.18(2)	0.07(4)	1.0[b)]
	O···D	2.04(3)	0.11(5)	2.0[b)]
D_2O	O–D	0.984(2)	0.064(2)	2.0[b)]
	D···D	1.546(9)	0.124(8)	1.0[b)]
Hydrogen bond	O···D	1.92(2)	0.22(2)	1.9(2)
	D···D	2.42(2)	0.24(3)	6.2(6)
$Na^+\cdots D_2O$	Na···O	2.5(5)	0.3(3)	4.0[b)]
	Na···D	2.9(2)	0.2(1)	8.0[b)]

a) Estimated standard deviations are given in the parentheses. b) Fixed.

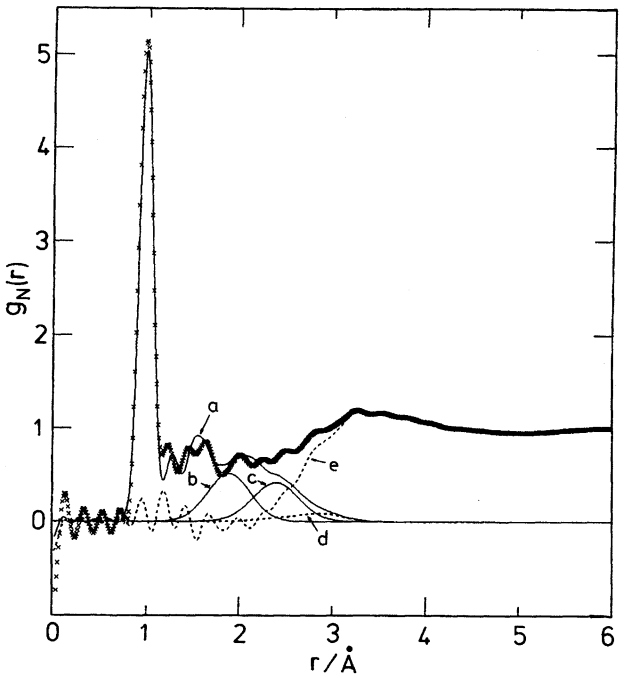

Fig. 2. The neutron total distribution function, $g_N(r)$, (crosses) and the Fourier transform of the model function, $i_N^{calc}(Q)$, (solid line-a) which is composed of intramolecular contribution from $DCOO^-$ and D_2O molecules and short range intermolecular O···D (solid line-b), D···D (solid line-c), and $Na^+\cdots O$+$Na^+\cdots D$ (dotted line-d) pairs. The Fourier transform of the difference, $i_N(Q)-i_N^{calc}(Q)$, is denoted by the dotted line-e.

and those in gaseous formic acid (r_{CH}=1.09—1.10 Å[27,28]). The bond angles within $DCOO^-$ ($\angle$OCO=118±3°, $\angle$DCO=121±4°), calculated from the present r_{CD}, r_{CO}, r_{OO}, and r_{OD} values, apparently indicate a planer molecular structure of the formate ion in aqueous solution. The structural parameters for the D_2O molecule in an aqueous 15 mol% DCOONa solution is in complete agreement with those reported in pure liquid D_2O within the experimental error,[13,29] implying that the structure of the D_2O molecule remains unchanged in such a concentrated DCOONa solution. Further, the present intermolecular hydrogen-bond distances (r(O···D)=1.92±0.02 Å, r(D···D)=2.42±0.02 Å) are almost identical to those reported in pure liquid water (r(O···D)=1.9 Å, r(D···D)=2.4 Å).[30,31] The coordination number (n(O···D)), determined in the present analysis, is close to 2, suggesting that a tetrahedral hydrogen-bonded network among H_2O molecules exists in solution. It may be difficult to discuss the $Na^+\cdots D_2O$ correlation by employing only neutron data, because this correlation has only a small contribution to the total $i_N(Q)$. The hydration structure of Na^+ in solution is discussed later based on the X-ray and Raman spectroscopic data.

The observed total X-ray interference term ($i_X(Q)$) and the X-ray total-distribution function ($g_X(r)$) are shown in Figs. 3a and 4a, respectively. A sharp peak located at $r\approx$1.3 Å in $g_X(r)$ can be assigned to the intramolecular C–O interaction within $HCOO^-$. Unphysical ripples appearing around this peak may be due to a termination effect in the Fourier transform. In order to obtain more definitive information on the nearest-neighbor intermolecular structure in solution, we subtracted the calculated intramolecular interference term for both the $HCOO^-$ and H_2O molecules (denoted by the solid line in Fig. 3a) from the observed total-interference term ($i_X(Q)$). In the calculation, the intramolecular parameters for the formate ion and water molecule were all fixed at values which had already been determined from the present neutron data. Figures 3b and 4b represent the intermolecular interference term ($i_X^{inter}(Q)$) and its Fourier transform ($g_X^{inter}(r)$), respectively. The fact that the value of $g_X^{inter}(r)\approx 0$ in the $r<2$ Å range maybe evidence that the correction and normalization procedures have been properly applied in the present data analysis. The termination ripples associated with the intramolecular C–O peak in the total $g_X(r)$ is significantly reduced in the $g_X^{inter}(r)$ function. Although the functional form $g_X^{inter}(r)$ appears to be relatively featureless, the peaks at r=2.4 and 2.8 Å remain at a certain position when varying the value of the upper limit (Q_{max}) on the Fourier transform. These peaks are therefore considered to reflect a real structure, and are not the consequence of a termination error. The

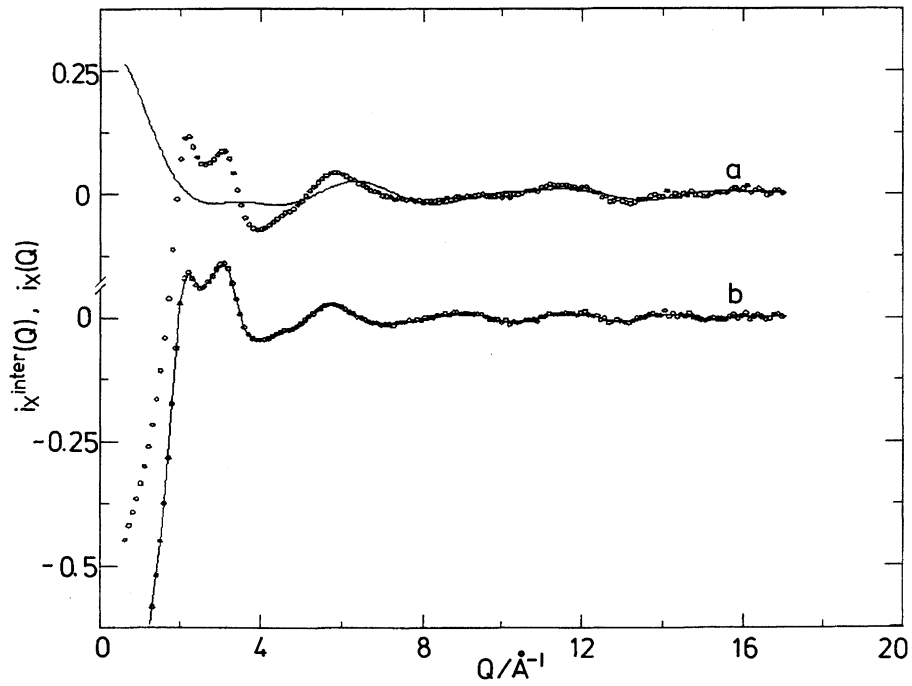

Fig. 3. (a) Circles: The observed X-ray total interference term, $i_X(Q)$, for the 15 mol% HCOONa solution in H_2O. Solid line: The calculated intramolecular contributions from $HCOO^-$ and H_2O molecules. (b) Circles: The observed intermolecular interference term, $i_X^{inter}(Q)$. Solid line: Smoothed $i_X^{inter}(Q)$ used for the Fourier transform.

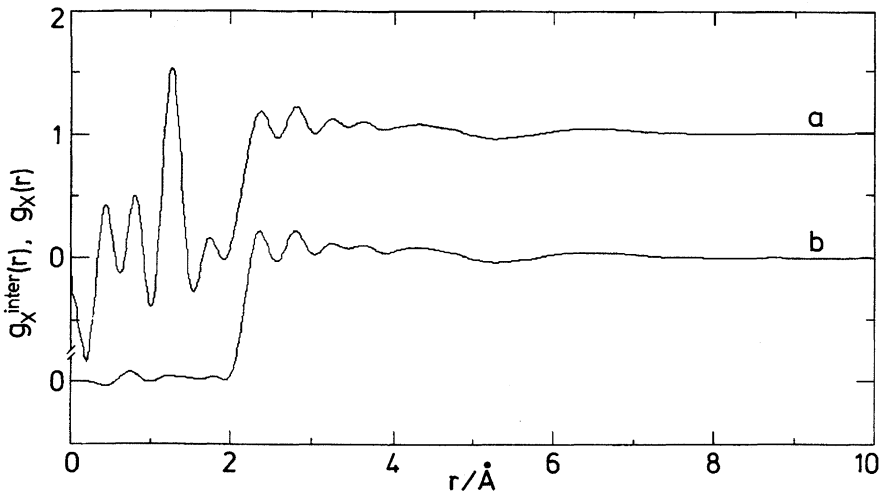

Fig. 4. The X-ray total (a) and intermolecular (b) distribution functions for the 15 mol% HCOONa solution in H_2O.

peak located at r=2.4 Å may be attributed to the nearest-neighbor $Na^+\cdots H_2O$ interaction. This peak position is almost equivalent to the sum of the ionic radius of Na^+ (1.0 Å[32]) and the effective radius of H_2O molecule (1.4 Å) in aqueous solution.[33] The peak at r=2.8 Å can be ascribed to the hydrogen-bonded $H_2O\cdots H_2O$ interaction. The nearest-neighbor $O_{formate}\cdots H_2O$ interaction may be involved in this peak. The features appearing at $r\approx$3.5 and 4.5 Å in $g_X^{inter}(r)$ may indicate the existence of some preferred orientation between $HCOO^-$ and the neighboring water molecules in the solution.

We next performed a least-squares fitting analysis for $i_X^{inter}(Q)$, in light of information from the experimental $g_X^{inter}(r)$ in order to determine the structural parameters of the nearest-neighbor intermolecular correlation (r_{ij}, l_{ij}, and n_{ij}). The following assumptions were employed in evaluating the theoretical interference terms: (a) The correlation between Na^+ and H_2O molecule in the first hydration shell can be calculated by two different models. In the first model, the intermolecular distance ($r_{Na\cdots H_2O}$), its root-mean-square displacement ($l_{Na\cdots H_2O}$), and the coordination number ($n_{Na\cdots H_2O}$) are allowed to vary independently. In another model, the tetrahedral hydration geometry around Na^+ ($n_{Na\cdots H_2O}$=4, fixed) is adopted, introducing the $H_2O\cdots H_2O$ interaction in the coordination polyhedron around Na^+, in which the parameters ($r_{Na\cdots H_2O}$ and $l_{Na\cdots H_2O}$) are both re-

fined as being independent. In this model, the intermolecular distance within the $Na^+(H_2O)_4$ unit ($r_{H_2O\cdots H_2O}$) was evaluated from the value of $r_{Na\cdots H_2O}$ through the relation $r_{H_2O\cdots H_2O}=(8/3)^{1/2}\cdot r_{Na\cdots H_2O}$, while its root-mean-square displacement ($l_{H_2O\cdots H_2O}$) was allowed to vary independently. (b) Hydrogen-bonded interaction parameters between the bulk H_2O molecules ($r_{H_2O\cdots H_2O}$, $l_{H_2O\cdots H_2O}$, and $n_{H_2O\cdots H_2O}$) were refined so as to vary independently. (c) The interaction between the formate ion and the nearest-neighbor water molecules was taken into account in the following manner: i) The nearest-neighbor bond distance ($r_{O_{formate}\cdots H_2O}$), its root-mean-square displacement ($l_{O_{formate}\cdots H_2O}$), and the coordination number ($n_{O_{formate}\cdots H_2O}$) were treated as independent parameters. ii) The independent parameters, dihedral angle α between the molecular plane of $HCOO^-$ and the plane involving C, $O_{formate}$, and H_2O, and the bond angle β ($=\angle C\text{–}O_{formate}\cdots H_2O$) were introduced in order to determine the configuration of $HCOO^-\cdots H_2O$ complex, and to calculate the non-bonded interatomic distances within the complex. iii) The root-mean-square displacement for the non-bonded interaction within the $HCOO^-\cdots H_2O$ complex (l_{ij}) was approximated using the following equation:[15]

$$l_{ij} = l_{O_{formate}\cdots H_2O}\cdot(r_{ij}/r_{O_{formate}\cdots H_2O})^{1/2}, \quad (23)$$

where r_{ij} denotes the calculated intermolecular distance.

Since the nearest-neighbor $Na^+\cdots H_2O$, $H_2O\cdots H_2O$, and $O_{formate}\cdots H_2O$ distances are rather similar to each other, it is generally difficult to carry out a least-squares fit without any assumption concerning initial values, which are applied in the calculation. We therefore inserted initial values ($r_{Na\cdots H_2O}=2.4$ Å, $r_{H_2O\cdots H_2O}=2.8$ Å and $r_{O_{formate}\cdots H_2O}=2.8$ Å), which were suggested from the present $g_X^{inter}(r)$ function. A reliable determination for the long-range parameters may be more difficult. The initial value of the distance parameter (r_{0ij}) was taken to be 3.0 Å for all of the atom pairs in the structure model, assuming $n_{Na\cdots H_2O}$=free. For a structure model involving a tetrahedral geometry of hydrated Na^+, the initial value of $r_{0ij}=5.0$ Å was applied for solute–solute interactions, while $r_{0ij}=3.0$ Å was adopted for solute–solvent and solvent–solvent interactions.

In Fig. 5, the theoretical interference term ($i_X^{inter}(Q)$) and the distribution function ($g_X^{inter}(r)$), obtained from the best fit of the first model ($n_{Na\cdots H_2O}$=free), are compared with the corresponding observed ones. A satisfactory agreement was obtained between the observed and calculated $i_X^{inter}(Q)$ in the $Q>4$ Å^{-1} range. The peaks at $r=2.4$ and 2.8 Å in the observed $g_X^{inter}(r)$ are well reproduced by the contributions from the nearest-neighbor $Na^+\cdots H_2O$ and $H_2O\cdots H_2O$+$O_{formate}\cdots H_2O$ interactions, respectively. The structural features appearing at $r\approx3.5$ and 4.5 Å in the experimental distribution function may be attributed to non-bonded interactions, $C\cdots H_2O$ and $O'_{formate}\cdots H_2O$, within the $HCOO^-\cdots H_2O$ complex. The double peak at $Q\approx3$ Å^{-1} in the observed $i_X^{inter}(Q)$ is not well reproduced, probably because the long-range water–water interactions (beyond the second nearest neighbor) are not taken into account in the present model function.[17] The final values of all independent parameters are summarized in Table 2. The present value of $r_{Na\cdots H_2O}$ ($=2.37\pm0.01$ Å) is in

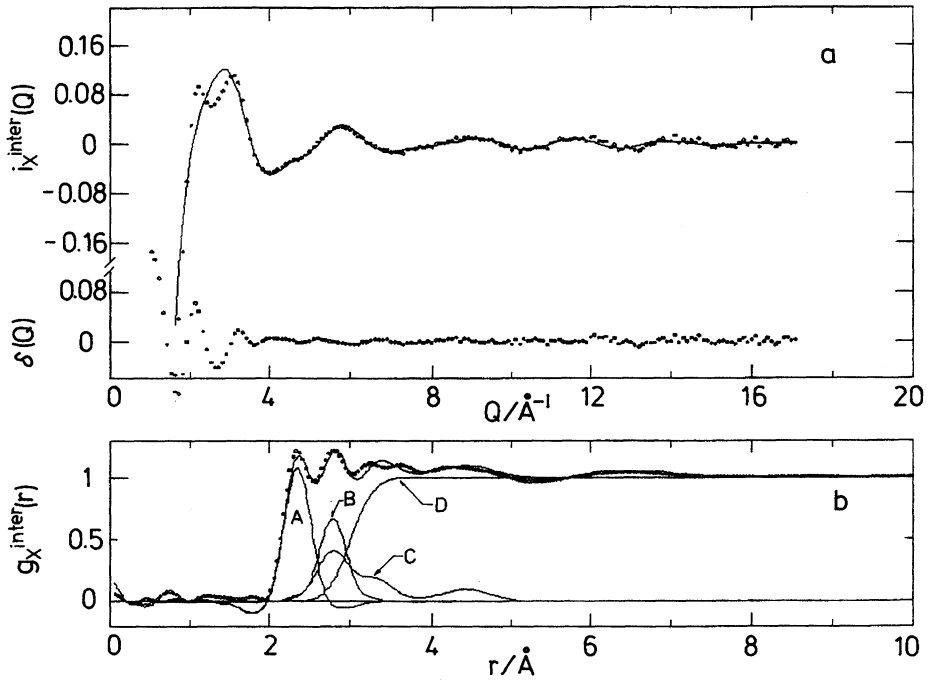

Fig. 5. (a) Circles: The observed X-ray intermolecular interference term, $i_X^{inter}(Q)$. Solid line: The calculated interference term, $i_X^{calc}(Q)$, with $n_{Na^+\cdots H_2O}$=free. The differences between $i_X^{inter}(Q)$ and $i_X^{calc}(Q)$ at $Q>1.0$ Å^{-1} are shown below. (b) Circles: The observed X-ray intermolecular distribution function, $g_X^{inter}(r)$. Solid line: The contributions from the nearest neighbor $Na^+\cdots H_2O$ (A), hydrogen-bonded $H_2O\cdots H_2O$ (B), $HCOO^-\cdots H_2O$ (C) pairs. The contribution from the long-range interaction is denoted by D.

Table 2. Results of the Least-Squares Refinements for the X-ray Intermolecular Interference Term of Aqueous 15 mol% HCOONa Solution[a)]

$n_{Na^+\cdots H_2O}$=free	Interaction	r_{ij}/Å	l_{ij}/Å	n_{ij}	α/°[g)]	β/°[h)]
Nearest neighbor	$Na^+\cdots H_2O$	2.37(1)	0.16(1)	4.6(2)		
	$H_2O\cdots H_2O$[e)]	2.81(1)	0.16(1)	1.9(1)		
	$O_{formate}\cdots H_2O$[f)]	2.82(2)	0.15(1)	4.4(2)	33(3)	103(2)
	Interaction	r_{0ij}/Å	l_{0ij}/Å			
Continuous	$Na^+\cdots H_2O$	3.0(1)	0.2(1)			
	$H_2O\cdots H_2O$	3.00(2)	0.18(3)			
	$HCOO^-\cdots H_2O$	2.98(3)	0.17(9)			
	$Na^+\cdots Na^+$	3.4(2)	0.3(2)			
	$HCOO^-\cdots Na^+$	3.0(1)	0.2(1)			
	$HCOO^-\cdots HCOO^-$	3.2(1)	0.3(1)			
$n_{Na^+\cdots H_2O}$=4	Interaction	r_{ij}/Å	l_{ij}/Å	n_{ij}	α/°[g)]	β/°[h)]
Nearest neighbor	$Na^+\cdots H_2O$	2.37(1)	0.16(1)	4[b)]		
	$H_2O\cdots H_2O$[c)]	3.87[d)]	0.47(6)	6.0[b)]		
	$O_{formate}\cdots H_2O$[f)]	2.77(1)	0.14(2)	4.8(2)	25(5)	104(2)
	$H_2O\cdots H_2O$[e)]	2.83(1)	0.13(1)	0.9(1)		
	Interaction	r_{0ij}/Å	l_{0ij}/Å			
Continuous	$Na^+\cdots H_2O$	2.95(6)	0.2(1)			
	$H_2O\cdots H_2O$	2.82(6)	0.54(8)			
	$HCOO^-\cdots H_2O$	3.01(2)	0.20(3)			
	$Na^+\cdots Na^+$	5.4(5)	0.7(2)			
	$HCOO^-\cdots Na^+$	4.5(2)	0.4(1)			
	$HCOO^-\cdots HCOO^-$	5.2(1)	0.3(1)			

a) Estimated standard deviations are given in the parentheses. b) Fixed. c) Interaction within the $Na^+(H_2O)_4$ unit. d) Calculated from $\sqrt{8/3}\cdot r_{Na^+\cdots H_2O}$. e) Interaction among the bulk water molecules. f) Interaction between formate oxygen and water molecule. g) Dihedral angle between molecular plane of $HCOO^-$ and the plane includes, C, $O_{formate}$, and H_2O. h) Bond angle, $\angle$C–$O_{formate}\cdots H_2O$.

good agreement with that reported by X-ray diffraction studies for various aqueous solutions containing Na^+.[8,17,34—38] The mean hydration number ($n_{Na\cdots H_2O}$=4.6±0.2) determined in this work, which agrees well with the value obtained for a saturated (6.18 mol kg^{-1}) NaCl solution,[17] may indicate that the coexistence of Na^+ ions which have a different number (4, 5 or 6) of the nearest-neighbor H_2O molecules, or an extended distribution of the hydration number of Na^+, may exist in a 15 mol% HCOONa solution. The present value of the intermolecular $H_2O\cdots H_2O$ distance ($r_{H_2O\cdots H_2O}$ (2.81±0.01 Å)) agrees well with that reported in pure liquid water.[30,38—41] The distance between the carboxyl oxygen of the formate ion and the nearest-neighbor H_2O molecule was determined to be 2.82±0.02 Å, in good agreement with the hydrogen-bond distance between the bulk water molecules in this solution, indicating the formation of a hydrogen bond between the carboxyl oxygen and the nearest-neighbor H_2O molecule. The hydration number of the formate ion was determined to be 4.4±0.2. The sum of the hydration number for solute ions in the present solution ($n_{Na\cdots H_2O}+n_{O_{formate}\cdots H_2O}$) is equal to 9.0, indicating that a considerable amount of the water-bridged ion pair ($Na^+\cdots H_2O\cdots HCOO^-$) may be formed in a 15 mol% HCOONa solution in which there are only 5.7 (=85/15) water molecules per one HCOONa. The dihedral angle (α) and the bond angle (β) were determined to be 33±3° and 103±2°, respectively. It may be considered that a preferred orientation between $HCOO^-$ and H_2O exists in the solution.

In order to examine the effect of introducing the $H_2O\cdots H_2O$ interaction within hydrated Na^+ in the structure model, we next carried out a least-squares fit using a model function involving the $H_2O\cdots H_2O$ interaction within the $Na^+(H_2O)_n$ structural unit, where n was assumed to be 4. In Fig. 6, the theoretical interference term ($i_X^{inter}(Q)$) and the distribution function ($g_X^{inter}(r)$), obtained from the best fit of the second model ($n_{Na\cdots H_2O}$=4), are compared with the corresponding observed one. A satisfactory agreement is again obtained between the observed and calculated $i_X^{inter}(Q)$. The final values of all the independent parameters are also given in Table 2. In this model, the agreement between the observed $i_X^{inter}(Q)$ and the calculated one was slightly improved in the $1<Q<4$ Å^{-1} range. However, the result of a least-squares fit indicated that a very large value of $l_{H_2O\cdots H_2O}$ (within the $Na^+(H_2O)_4$ unit) is necessary for an optimized fitting. This is probably because the calculated distance ($r_{H_2O\cdots H_2O}$ (=3.9 Å)) within the $Na^+(H_2O)_4$ unit falls on the shallow dip of the observed $g_X^{inter}(r)$. The large value of $l_{H_2O\cdots H_2O}$ may imply that a considerable fluctuation of the hydration geometry of Na^+ can exist in this solution. The final values for the bond distance between Na^+ and H_2O, the hydration number of $HCOO^-$ and its hydration geometry showed a reasonable agreement with the values determined using the first structural model assuming $n_{Na\cdots H_2O}$=free.

Figure 7 shows the low-frequency isotropic Raman spec-

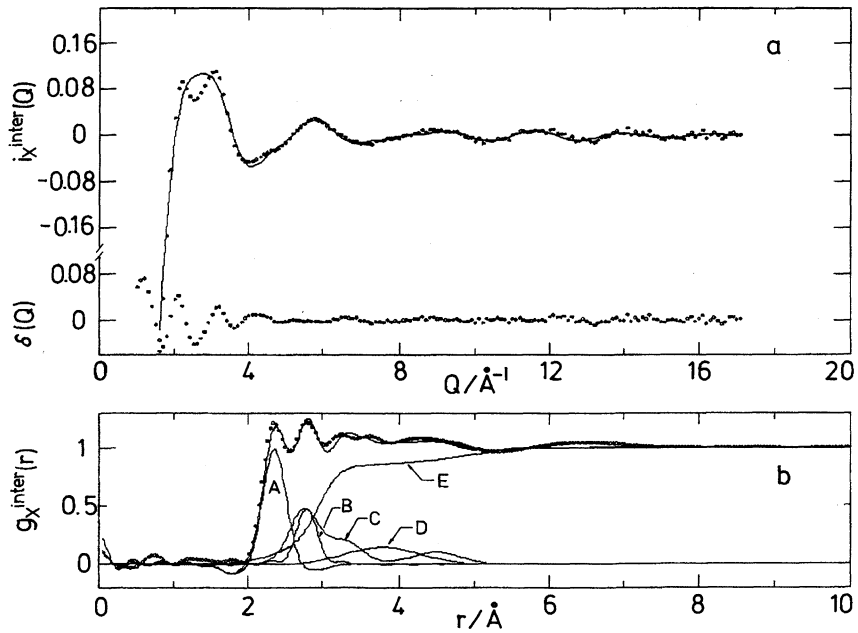

Fig. 6. (a) Circles: The observed X-ray intermolecular interference term, $i_X^{inter}(Q)$. Solid line: The calculated interference term, $i_X^{calc}(Q)$, with $n_{Na^+\cdots H_2O}$=4. The differences between $i_X^{inter}(Q)$ and $i_X^{calc}(Q)$ at $Q>1.0$ Å^{-1} are shown below. (b) Circles: The observed X-ray intermolecular distribution function, $g_X^{inter}(r)$. Solid line: The contributions from the nearest neighbor $Na^+\cdots H_2O$ (A), hydrogen-bonded $H_2O\cdots H_2O$ (B), $HCOO^-\cdots H_2O$ (C), and $H_2O\cdots H_2O$ pairs within $Na^+(H_2O)_4$ structural unit (D). The contribution from the long-range interaction is denoted by E.

tra in aqueous 5 and 15 mol% HCOONa solutions in H_2O and partially in D_2O. For the purpose of a comparison, the isotropic spectra in aqueous 5 and 10 mol% NaBr and NaCl solutions are also given in Fig. 7. A sharp Raman peak appearing at $\nu\approx770$ cm^{-1} in the HCOONa solution can be ascribed to the intramolecular COO deformation band ($\delta(CO_2)$) within $HCOO^-$.[42] Moreover, a broad polarized peak can be observed in the vicinity of 200 cm^{-1} in all spectra, the intensity of which increases with increasing the salt concentration. The position of this peak agrees well with that of the intermolecular stretching mode between neighboring H_2O molecules in pure liquid water.[21,43] However, this broad band appears to involve an alternative polarized component, because the $H_2O\cdots H_2O$ stretching mode in pure liquid water has been proved to have a purely depolarized nature.[43] Michaerian and Moskovits examined the low-frequency Raman spectra of aqueous NaCl and NaBr solutions by a difference method.[44] They found a completely polarized band at 170 cm^{-1} in both solutions, and assigned the band to the symmetric stretching vibrational mode of a tetrahedrally hydrated sodium ion, $Na^+(H_2O)_4$. One of the possible interpretations may be that the peak in the vicinity of 200 cm^{-1} observed in the present spectra contains the symmetrical stretching vibrational mode of the hydrated sodium ion, $Na^+(H_2O)_n$, which was commonly present in all of the solutions investigated in the present work.

$$\nu_{D_2O\ soln}/\nu_{H_2O\ soln}\approx(m_{H_2O}/m_{D_2O})^{1/2}=0.95. \quad (24)$$

If this might be the case, the ratio of the vibrational frequency of this mode between D_2O and H_2O solutions

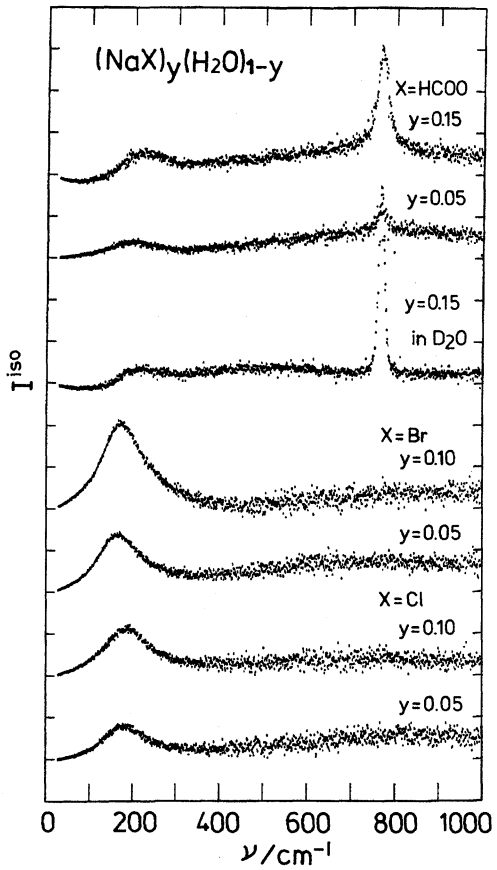

Fig. 7. Isotropic Raman spectra for aqueous HCOONa, NaBr, and NaCl solutions at 25 °C.

Table 3. The Observed Symmetrical Stretching Vibrational Frequency, ν_1, of $Na^+(H_2O)_n$ Structural Unit in Aqueous Solution $(NaX)_y(H_2O)_{1-y}$[a)]

X	y	ν_1/cm^{-1}
HCOO	0.15	225(2)
	0.05	190(4)
	0.15[b)]	219(2)
Br	0.10	172(1)
	0.05	164(1)
Cl	0.10	184(2)
	0.05	181(2)

a) Estimated standard deviations are given in the parentheses.
b) for D_2O solution.

can be approximated as follows,[44] considering the hydration geometry around Na^+ with n=4 (tetrahedral) or n=6 (octahedral): It appears that this value corresponds well to the ratio $\nu_{D_2O\ soln}/\nu_{H_2O\ soln}$=0.97±0.02 in an aqueous 15 mol% HCOONa solution. According to the X-ray diffraction result described above, the hydration number of Na^+ in this solution has been proven to be 4.6. The peak around $\nu\approx$200 cm^{-1} in the isotropic Raman spectrum in the 15 mol% HCOONa solution can be assigned to the totally symmetric stretching mode of the $Na^+(H_2O)_n$ (n=4 or 6) structural unit. The peak position derived from a Gaussian fit is listed in Table 3. It can be seen from the data that the peak frequency is strongly anion dependent. A similar anion dependence was observed in our previous work concerning the low-frequency isotropic Raman spectra of aqueous LiBr and LiCl solutions.[9] The relatively large composition dependence of the peak position in the sodium formate solution may indicate the effect of a solvent-shared ion pair, which is considered to be formed in a 15 mol% HCOONa solution.

The authors would like to thank Professors Masakatsu Misawa (Niigata University), Toshiharu Fukunaga (Nagoya University), and Tosio Yamaguchi (Fukuoka University) for their help during the course of the neutron-diffraction measurement. All of the calculations were carried out with the ACOS S3600 and EWS 4800 computers at the Computing Center of Yamagata University. This work was partially supported by a Grant-in-Aid for Scientific Research No. 06640712 from the Ministry of Education, Science and Culture.

References

1) C. Oldham, "Comprehensive Coordination Chemistry," ed by G. Wilkinson, Pergamon Press, Oxford (1987), Vol.2, p. 435.
2) H. G. M. Edwards and A. Knowles, *J. Mol. Struct.*, **268**, 13 (1992).
3) E. Spinner, *J. Chem. Soc. B*, **1967**, 879.
4) R. J. Bartholomew and D. E. Irish, *Can. J. Chem.*, **71**, 1728 (1993).
5) K. Ozutsumi, H. Ohtaki, and A. Kusumegi, *Bull. Chem. Soc. Jpn.*, **57**, 2612 (1984).
6) W. L. Jorgensen and J. Gao, *J. Phys. Chem.*, **90**, 2174 (1986).
7) T. Fukunaga, M. Misawa, I. Fujikura, and S. Satoh, "KENS REPORT-IX," (1993), p. 16.
8) Y. Kameda, R. Takahashi, T. Usuki, and O. Uemura, *Bull. Chem. Soc. Jpn.*, **67**, 956 (1994).
9) Y. Kameda, H. Ebata, and O. Uemura, *Bull. Chem. Soc. Jpn.*, **67**, 929 (1994).
10) Y. Kameda, I. Sugawara, K. Kijima, T. Usuki, and O. Uemura, *Bull. Chem. Soc. Jpn.*, **68**, 512 (1995).
11) H. H. Paalman and C. J. Pings, *J. Appl. Phys.*, **33**, 2635 (1962).
12) I. A. Blech and B. L. Averbach, *Phys. Rev.*, **137**, A1113 (1965).
13) Y. Kameda and O. Uemura, *Bull. Chem. Soc. Jpn.*, **65**, 2021 (1992).
14) T. Nakagawa and Y. Oyanagi, "Recent Developments in Statistical Inference and Data Analysis," ed by K. Matushita, North-Holland (1980), p. 221.
15) A. H. Narten, M. D. Danford, and H. A. Levy, *Discuss. Faraday Soc.*, **43**, 97 (1967).
16) R. Caminiti, P. Cucca, M. Monduzzi, G. Saba, and G. Crisponi, *J. Chem. Phys.*, **81**, 543 (1984).
17) H. Ohtaki and N. Fukushima, *J. Solution Chem.*, **21**, 23 (1992).
18) G. W. Chantry, "The Raman Effect," ed by A. Anderson, Marcel Dekker Inc., New York (1971), Vol. 1, p. 70.
19) J. R. Scherer, M. K. Go, and S. Kint, *J. Phys. Chem.*, **78**, 1304 (1974).
20) M. Lucas, A. De Trobriand, and M. Ceccaldi, *J. Phys. Chem.*, **79**, 913 (1975).
21) G. E. Walrafen, M. R. Fisher, M. S. Hokmabadi, and W.-H. Young, *J. Chem. Phys.*, **85**, 6970 (1986).
22) W. H. Zachariasen, *J. Am. Chem. Soc.*, **62**, 1011 (1940).
23) P. L. Markila, S. J. Retting, and J. Trotter, *Acta Crystallogr. Sect. B*, **B31**, 2927 (1975).
24) J. W. Bats and H. Fuess, *Acta Crystallogr., Sect. B*, **B36**, 1940 (1980).
25) B. F. Mentzen and Y. Odden, *Inorg. Chim. Acta*, **43**, 237 (1980).
26) H. Bertagnolli, P. Chieux, and H. G. Hertz, *Ber. Bunsenges. Phys. Chem.*, **88**, 977 (1984).
27) A. M. Mirri, *Nuovo Cimento*, **18**, 849 (1960).
28) M. R. Peterson and I. G. Csizmadia, *J. Am. Chem. Soc.*, **101**, 1076 (1979).
29) J. G. Powles, *Mol. Phys.*, **42**, 757 (1981).
30) A. K. Soper and M. G. Phillips, *Chem. Phys.*, **107**, 47 (1986).
31) A. K. Soper, *J. Chem. Phys.*, **101**, 6888 (1994).
32) R. D. Shannon, *Acta Crystallogr., Sect. A*, **A32**, 751 (1976).
33) Y. Marcus, *Chem. Rev.*, **88**, 1475 (1988).
34) M. Maeda and H. Ohtaki, *Bull. Chem. Soc. Jpn.*, **48**, 3755 (1976).
35) G. Pálinkás, W. O. Ried, and K. Heinzinger, *Z. Naturforsch. A*, **32a**, 1137 (1977).
36) R. Caminiti, G. Licheri, G. Paschina, G. Piccaluga, and G. Pinna, *J. Chem. Phys.*, **72**, 4522 (1980).
37) R. Caminti, F. Cilloco, and R. Felici, *Mol. Phys.*, **76**, 681 (1992).
38) A. H. Narten and H. A. Levy, *J. Chem. Phys.*, **55**, 2263 (1971).
39) G. A. Gaballa and G. W. Neilson, *Mol. Phys.*, **50**, 97 (1983).
40) R. Corban and M. D. Zeidler, *Ber. Bunsenges. Phys. Chem.*, **96**, 1463 (1992).

41) A. V. Okhulkov, Yu. N. Demianets, and Yu. E. Gorbaty, *J. Chem. Phys.*, **100**, 1578 (1994).
42) J. D. Donaldson, J. F. Knifton, and S. D. Ross, *Spectrochim. Acta*, **21**, 1043 (1965).
43) M. Moskovits and K. H. Michaelian, *J. Chem. Phys.*, **69**, 2306 (1978).
44) K. H. Michaelian and M. Moskovits, *Nature*, **273**, 135 (1978).